



# Alpha-1-B glycoprotein (A1BG) inhibits sterol-binding and export by CRISP2

Received for publication, March 26, 2024, and in revised form, October 4, 2024 Published, Papers in Press, October 19, 2024,  
<https://doi.org/10.1016/j.jbc.2024.107910>

Ola El Atab<sup>1</sup>, Barkha Gupta<sup>1</sup>, Zhu Han<sup>1</sup>, Jiri Stribny<sup>1</sup>, Oluwatoyin A. Asojo<sup>2</sup>, and Roger Schneider<sup>1,\*</sup>

From the <sup>1</sup>Department of Biology, University of Fribourg, Chemin du Musée 10, Fribourg, Switzerland; <sup>2</sup>Dartmouth Cancer Center, Lebanon, New Hampshire, United States

Reviewed by members of the JBC Editorial Board. Edited by Henrik Dohlman

Proteins belonging to the CAP superfamily are present in all kingdoms of life and have been implicated in various processes, including sperm maturation and cancer progression. They are mostly secreted glycoproteins and share a unique conserved CAP domain. The precise mode of action of these proteins, however, has remained elusive. *Saccharomyces cerevisiae* expresses three members of this protein family, which bind sterols *in vitro* and promote sterol secretion from cells. This sterol-binding and export function of yeast Pry proteins is conserved in the mammalian cysteine-rich secretory protein (CRISP) proteins and other CAP superfamily members. CRISP3 is an abundant protein of the human seminal plasma and interacts with alpha-1-B glycoprotein (A1BG), a human plasma glycoprotein that is upregulated in different types of cancers. Here, we examined whether the interaction between CRISP proteins and A1BG affects the sterol-binding function of CAP family members. Coexpression of A1BG with CAP proteins abolished their sterol export function in yeast and their interaction inhibits sterol-binding *in vitro*. We map the interaction between A1BG and CRISP2 to the third of five repeated immunoglobulin-like domains within A1BG. Interestingly, the interaction between A1BG and CRISP2 requires magnesium, suggesting that coordination of Mg<sup>2+</sup> by the highly conserved tetrad residues within the CAP domain is essential for a stable interaction between the two proteins. The observation that A1BG modulates the sterol-binding function of CRISP2 has potential implications for the role of A1BG and related immunoglobulin-like domain containing proteins in cancer progression and the toxicity of reptile venoms containing CRISP proteins.

The CAP domain constitutes the defining feature of a large protein superfamily with members found in all kingdoms of life. This superfamily derives its name from its founding constituents: Cysteine-rich secretory proteins (CRISPs) within the mammalian reproductive tract, antigen 5 (Ag5) within the venom secretory ducts of stinging insects, and pathogenesis-related protein-1 (PR-1), which is induced in plants upon pathogen infection (1–3). Additionally known as sperm coating proteins or TAPS (Tpx-1/Ag5/PR-1/Sc7), these

proteins share a conserved CAP domain characterized by a stable three-layered  $\alpha\beta\alpha$  sandwich fold (4). Central to this domain are tandem histidine residues flanked by acidic amino acid side chains (Glu-His, Glu-His), known as tetrad residues, which coordinate binding of a divalent cation such as Zn<sup>2+</sup> or Mg<sup>2+</sup> (5–8). CAP superfamily members are mostly secreted glycoproteins and have been implicated in many fundamental biological processes including immune defense in mammals and plants, sperm maturation and fertilization, prostate and brain cancer, pathogen virulence, and venom toxicity. Even though these proteins are extensively studied, their precise mode of action remains to be defined (1–3, 9, 10).

CRISP2 is a notable member of the CRISP family, predominantly associated with male reproductive biology, and plays an essential role in sperm maturation and fertilization (1, 11, 12). Mammalian CRISP proteins typically comprise an N-terminal CAP domain and a C-terminal cysteine-rich domain, also referred to as ion channel regulatory domain, linked by a hinge region (13–15). Dysregulation of certain CRISP proteins in malignant cells hints at their potential roles in cancer progression; for instance, CRISP3 is significantly upregulated in prostate cancer, where it serves as a diagnostic and prognostic marker, and cholesterol has a likely role in the progression to advanced disease (16, 17). CRISP-like proteins found in reptiles and insect venoms exhibit neurotoxin-like effects and block angiogenesis, highlighting their diverse functionalities (18).

Alpha-1-B glycoprotein (A1BG) is a human plasma glycoprotein of unknown function (19, 20). The protein harbors five repeating structural domains of about 92 to 98 amino acids each, with sequence similarity to the variable region of members of the immunoglobulin (Ig) superfamily (21). A1BG is thus a member of the Ig superfamily, which serves diverse functions based on molecular recognition especially in the immune system and cell adhesion (22, 23). A1BG has been identified as an autoantigen in patients with rheumatoid arthritis and is overexpressed in rheumatoid arthritis, pancreatic ductal adenocarcinoma, bladder, breast and lung cancer, pediatric patients with steroid resistant nephrotic syndrome and liver cancer cell lines, suggesting that A1BG might be a cancer associated gene and a novel tumor marker (24–30). The glycosylation pattern of A1BG has been suggested to play a crucial role in its functional diversity,

\* For correspondence: Roger Schneider, [roger.schneider@unifr.ch](mailto:roger.schneider@unifr.ch).

## A1BG inhibits sterol-binding by CRISP2

influencing interactions with other proteins and cellular compartments (26, 31). Despite its association with various health conditions, the specific molecular mechanisms underlying A1BG's participation in these processes remain incompletely understood.

CRISP3 has been shown to bind A1BG with nanomolar affinity, forming a stable, noncovalent, equimolar stoichiometric complex (32). Complex formation between A1BG and CRISP3 appears to be conserved as serum A1BG across different mammals, including cow, horse, and rabbit, all bind human CRISP3, suggesting potential functional significance (33). The sterol-binding function of CRISP proteins has been implicated in cholesterol metabolism and cancer progression (34, 35). However, the precise role of A1BG, a known interactor of CRISP proteins, in modulating this function remains unexplored. This study aims to characterize the inhibitory effect of A1BG on CRISP2 sterol-binding and export and investigate the molecular basis of this interaction. We demonstrate that coexpression of A1BG with CRISP2 or CRISP3 impedes the sterol export function of CRISP proteins *in vivo* without affecting their secretion. Furthermore, purified A1BG binds CRISP2 with nanomolar affinity and inhibits sterol binding by CRISP2 *in vitro*. Our structural analysis suggests that the third Ig domain of A1BG (Ig3) engages in high-affinity binding with CRISP2, potentially *via* intermolecular antiparallel  $\beta$ -sheet interactions. Notably, the interaction between A1BG and CRISP2 requires magnesium, indicating the significance of magnesium coordination by the conserved tetrad residues within the CAP domain of CRISP2. We discuss the potential implications of this protein interaction in prostate physiology and an innate immunity against reptile venoms.

## Results

### Expression of A1BG blocks sterol export without affecting the secretion of CRISP2

To test for sterol binding and export by CAP family proteins, we use an *in vivo* sterol export assay that is based on yeast cells, which are deficient for heme synthesis (34). Heme-deficient *Saccharomyces cerevisiae* mutants (*hem1 $\Delta$* ) are unable to synthesize ergosterol, the main sterol made by fungal cells, and instead become auxotrophic for sterols (36, 37). This allows for labeling of membrane sterols in *hem1 $\Delta$*  deficient cells by providing radiolabeled [<sup>14</sup>C]-cholesterol in the culture media. Within the cells, the radiolabeled cholesterol is then subject to an acetylation/deacetylation cycle controlled by the alcohol acetyltransferase 2 and the sterol deacetylase Say1 (38). In the absence of the sterol deacetylase Say1 (*say1 $\Delta$* ), cholesterol acetate (CA) accumulates and gets eliminated through binding to the yeast CAP family members Pry1 and Pry2, followed by their excretion through the secretory pathway. Thus, in heme-deficient *say1 $\Delta$  pry1 $\Delta$  pry2 $\Delta$*  mutant cells, radiolabeled CA accumulates within the cells rather than in the culture supernatant (34). This block in secretion of acetylated sterols is relieved by expression of mammalian CAP family proteins, such as CRISP2 or CRISP3 (34). This

experimental set-up thus allows to test whether proteins that interact with CRISP family members interfere with their sterol binding and export function (35) (Fig. 1A).

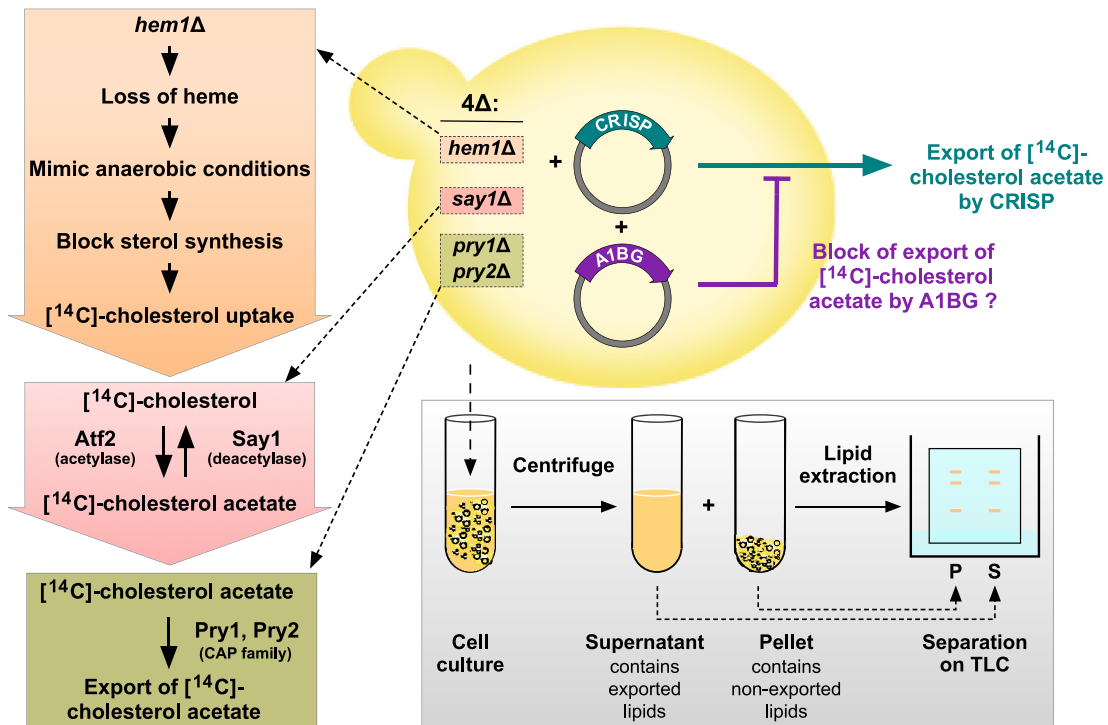
To examine whether the expression of A1BG would affect the sterol binding and export function of CRISP proteins, a plasmid driving expression of A1BG was transformed into quadruple mutant cells (44) lacking Hem1, Say1, Pry1, and Pry2. Cells were then radiolabeled in media containing [<sup>14</sup>C]-cholesterol, washed, and cultured in media containing unlabeled cholesterol to allow for export of acetylated [<sup>14</sup>C]-cholesterol into the culture supernatant. Lipids were then extracted from both the cell pellet and the culture supernatant and separated by TLC (Fig. 1B). Radiolabeled lipids were quantified, and the level of acetylated sterols present in the culture supernatant as a fraction of acetylated sterols present in both the cell pellet and the media were plotted as an export index (Fig. 1C). These experiments revealed that the coexpression of A1BG with either Pry1, CRISP3, or CRISP2 resulted in a block in sterol secretion by >50% (Fig. 1, B and C).

To assess whether expression of A1BG would affect the synthesis or secretion of either Pry1, CRISP3, or CRISP2, we coexpressed FLAG-tagged A1BG with hemagglutinin (HA)-tagged Pry1, CRISP3, or CRISP2, then separated yeast cells from the culture medium, precipitated proteins from both fractions with trichloroacetic acid (TCA) and detected the tagged proteins by Western blotting. While HA-tagged Pry1 was detected as a high molecular mass glycoform in the culture supernatant, CRISP2 and CRISP3 were detected in both the cell pellet and the culture supernatant (34). FLAG-tagged A1BG expressed as a fusion with an N-terminal signal peptide derived from pre-pro alpha mating pheromone was present as a high molecular pre-pro form in the culture supernatant, indicating that the protein is indeed secreted (Fig. 1D). Our results demonstrate that A1BG inhibits the sterol export function of different CAP family members, including Pry1, CRISP3, and CRISP2, suggesting a conserved regulatory mechanism across species that may play a critical role in cholesterol homeostasis. This effect occurs without impacting CRISP2 synthesis or secretion, highlighting a targeted inhibition of sterol-binding functionality.

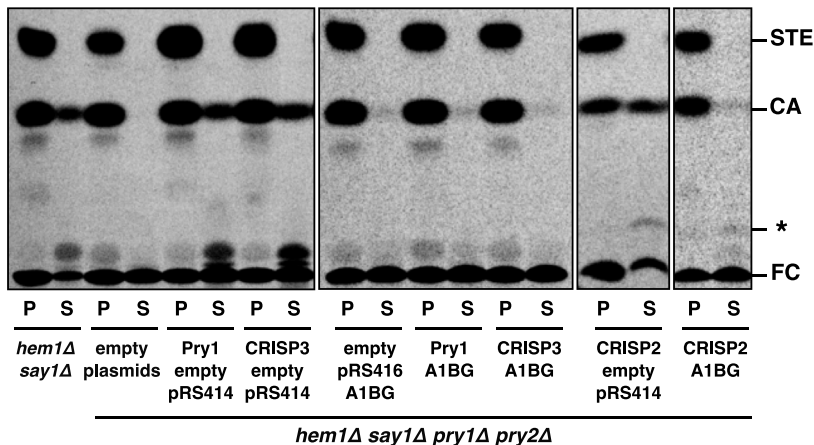
### A1BG binds CRISP2 with high affinity and inhibits sterol binding

To confirm a direct interaction of A1BG with CRISP2, we performed an *in vitro* protein binding assay using microscale thermophoresis (MST). MST was chosen due to its ability to precisely measure binding affinities in real time, even at low protein concentrations, making it ideal for studying interactions like that between A1BG and CRISP2. MST is based on the diffusion of a fluorescently labeled molecule along a microscopic temperature gradient. In this assay, the free protein diffuses faster than its ligand-bound form. Ligands can range from small ions to low molecular weight compounds, liposomes, and even entire viruses (35, 39–41). Purified and fluorescently labeled CRISP2 was incubated with varying concentrations of A1BG and the interaction between the two

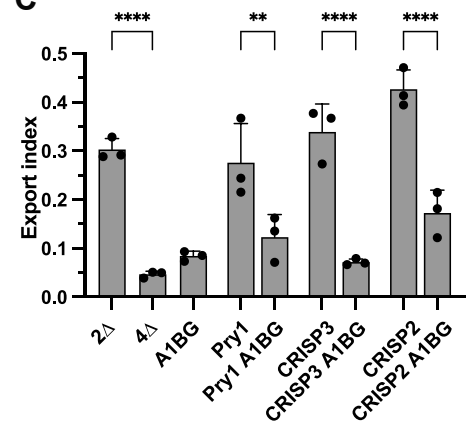
A



B



C



D

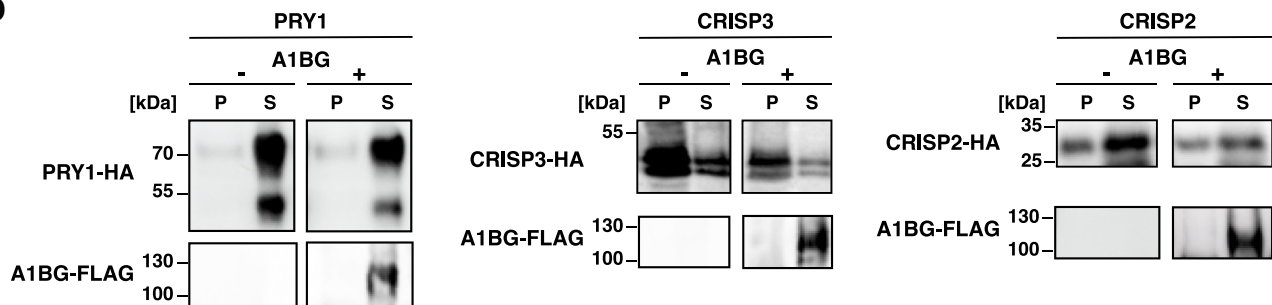


**Figure 1. A1BG inhibits sterol export by CAP family proteins.** A, schematic representation of the experimental system. Heme-deficiency of *Saccharomyces cerevisiae* mimics anaerobic conditions and allows for labeling of cells with exogenously supplied [ $^{14}\text{C}$ ]-cholesterol. Deletion of the sterol deacetylase Say1 results in the accumulation of acetylated [ $^{14}\text{C}$ ]-cholesterol, which is then secreted out of the cells by binding to the yeast CAP proteins Pry1 and Pry2. The block of secretion of [ $^{14}\text{C}$ ]-cholesterol acetate of a quadruple mutant ( $4\Delta$ ;  $hem1\Delta say1\Delta pry1\Delta pry2\Delta$ ) is complemented by a plasmid-borne copy of a mammalian CAP family proteins such as CRISP. Coexpression of a protein which interacts with CRISP, such as A1BG is being used to assess whether this protein-protein interaction (CRISP-A1BG) affects the sterol binding and export function of CRISP. B, export of acetylated cholesterol is blocked in cells expressing A1BG. Acetylation and export of [ $^{14}\text{C}$ ]-cholesterol was examined in  $hem1\Delta say1\Delta$  double mutant cells and in quadruple mutant cells

## A1BG inhibits sterol-binding by CRISP2

proteins was monitored by MST. The results show that A1BG binds CRISP2 with nanomolar affinity ( $K_d$  13.72  $\pm$  2.5 nM) (Fig. 2A), which is in accordance with the nanomolar affinity previously determined for the interaction between A1BG and CRISP3 by surface plasmon resonance ( $K_d$  2.1 nM) (32).

To test whether the interaction between A1BG and CRISP2 affects sterol-binding by CRISP2 *in vitro*, we performed lipid binding assays using a water-soluble cholesterol derivative, cholesterol sulfate. While CRISP2 bound cholesterol sulfate in the micromolar range ( $K_d$  3.21  $\pm$  1.22  $\mu$ M) as reported before (35), A1BG did not (Fig. 2, B and C). In the presence of an equimolar concentration of A1BG, however, sterol-binding by CRISP2 was blocked (Fig. 2D). These results show that complex formation between A1BG and CRISP2 inhibits the propensity of CRISP2 to accommodate sterols, suggesting that, under physiological conditions, A1BG could act as a modulator of lipid binding by CRISP2.

### A1BG does not affect the propensity of CRISP2 to bind and export fatty acids

CAP family proteins have previously been shown to bind eicosanoids and free fatty acids at a second lipid binding site that is independent of their sterol binding site (42–44). This fatty acid binding site is conserved in CRISP2, and we have previously shown that CRISP2 can export fatty acids *in vivo* (35) (Fig. S1A). To test whether A1BG affects fatty acid binding by CRISP2, we measured the affinity of CRISP2 and that of A1BG to palmitic acid by MST. While A1BG did not bind palmitic acid, CRISP2 bound this ligand with micromolar affinity ( $K_d$  64.6  $\pm$  20.7  $\mu$ M) (Fig. S1, B and C). This binding affinity of CRISP2 for palmitic acid was not significantly reduced in the presence of A1BG ( $K_d$  70.0  $\pm$  22.7  $\mu$ M), indicating that A1BG interferes with sterol binding of CAP family proteins, but not with their propensity to bind fatty acids (Fig. S1D).

These results were corroborated using an independent *in vivo* fatty acid binding and export assay. This assay is based on the observation that cells lacking the two major acyl-CoA synthases, Faa1 and Faa4, secrete free fatty acids into the medium (45). This lipid export depends on the presence of CAP proteins and is strongly reduced in cells lacking two of the yeast CAP proteins, Pry1 and Pry3 (44, 46). This block in fatty acid export in quadruple mutant cells (*faa1 $\Delta$  faa4 $\Delta$  pry1 $\Delta$  pry3 $\Delta$* ) is relieved by expression of either Pry1 or CRISP2 and is not impeded by the presence of A1BG, confirming that A1BG does not interfere with the propensity of CRISP2 to bind and export fatty acids (Fig. S1E). Taken together, these results suggest that A1BG

specifically affects the sterol binding site of the CAP domain but not the fatty acid binding pocket.

### *In silico* dockings predict strong interactions between the Ig3 domain of A1BG and CRISP2

To analyze the nature of the molecular interaction between A1BG and CRISP2 in more detail, we performed *in silico* protein docking experiments. Since no experimentally determined structural data for either A1BG or CRISP2 is available, we used AlphaFold2 (<https://alphafold.ebi.ac.uk/>) to predict the structure of the CAP domain of CRISP2, without its C-terminal channel regulatory domain (47). The predicted structure of the CAP domain of CRISP2 is similar to experimentally determined structures of other CAP family members such as the CAP domain of yeast Pry1 or that of tomato PR1, with RMSD values of 0.773 Å and 0.886 Å, respectively (4, 8). The CAP domain of CRISP2 harbors a conserved surface groove known as the CAP cavity with the tetrad residues implicated in coordinating divalent cations (Fig. 3A). In agreement with the sequence homology of A1BG to variable regions of immunoglobulin light and heavy chains, A1BG is predicted to harbor five Ig domains (Ig1–Ig5) and adopt an overall ring-shaped structure (21) (Fig. 3A). The Ig domains predicted by AlphaFold2 adopt the characteristic  $\beta$ -sheet fold of Ig superfamily members with a common structural core of 4  $\beta$ -strands within an antiparallel curled  $\beta$ -sheet sandwich (22). *In silico* dockings between the CAP domain of CRISP2 and A1BG revealed interactions between multiple Ig domains of A1BG and CRISP2 (Fig. 3B). Analysis of direct surface-to-surface interactions between these Ig domains and CRISP2 indicate that the Ig3 domain of A1BG displays the largest interaction surface, followed by interactions with Ig1 and Ig5 (Fig. 3, C and D). Consistent with data obtained from a PRODIGY analysis (PROtein binDing energy prediction), which determines the affinity of protein-protein interactions by predicting its Gibbs free energy ( $\Delta G$ ) and dissociation constant ( $K_d$ ), the interaction between Ig3 and CRISP2 is predicted to result in the lowest  $\Delta G$  and  $K_d$  ( $\Delta G$  = –11.1 kcal/mol and  $K_d$  = 7.7 nM, Fig. 3D). These results suggest that the Ig3 domain of A1BG provides the largest contribution to the interaction between the two proteins.

### The third Ig repeat domain of A1BG affects sterol binding by Pry1 and CRISP2 *in vivo*

To corroborate these *in silico* docking predictions, we expressed each one of the five Ig domains of A1BG

lacking the endogenous CAP family members Pry1 and Pry2 (*hem1 $\Delta$  say1 $\Delta$  pry1 $\Delta$  pry2 $\Delta$* ). Strains expressing the indicated CAP proteins (PRY1, CRISP3, or CRISP2) from a plasmid (pRS416) and coexpressing A1BG or bearing an empty control plasmid (pRS414) were cultivated in the presence of [<sup>14</sup>C]-cholesterol. Lipids were extracted from cell pellet (P) and culture supernatant (S), separated by TLC, and visualized by phosphorimaging. The position of free cholesterol (FC), cholesterol acetate (CA), sterol esters (STE), and an unidentified lipid (\*) are indicated to the right. C, quantification of cholesterol acetate export. The export index represents the relative levels of cholesteryl acetate exported by cells. Export inhibition by A1BG was consistent across three independent experiments, indicating a robust and reproducible interaction between A1BG and CAP family proteins. Data correspond to means  $\pm$  S.D. of 3 independent experiments and statistical significance is indicated: \*\* $p$   $\leq$  0.01; \*\*\*\* $p$   $\leq$  0.0001 (one-way ANOVA with Tukey's *post hoc* test). Precise  $p$ -values of all statistical analyses are given in Tables S1. D, expression of A1BG does not block the synthesis or secretion of CAP family members. Proteins were TCA precipitated from the cell pellet (P) and the culture medium (S) of cells expressing HA-tagged Pry1, CRISP2, or CRISP3 in the presence (+) or absence (–) of FLAG-tagged A1BG and analyzed by Western blotting. Pry1 is detected as a high molecular weight glycosylated protein in the culture supernatant. A1BG fused to the N-terminal signal sequence of pre-pro alpha factor is present as a pre-pro form in the culture supernatant. A1BG, alpha-1-B glycoprotein; CRISP, cysteine-rich secretory protein; TCA, trichloroacetic acid.

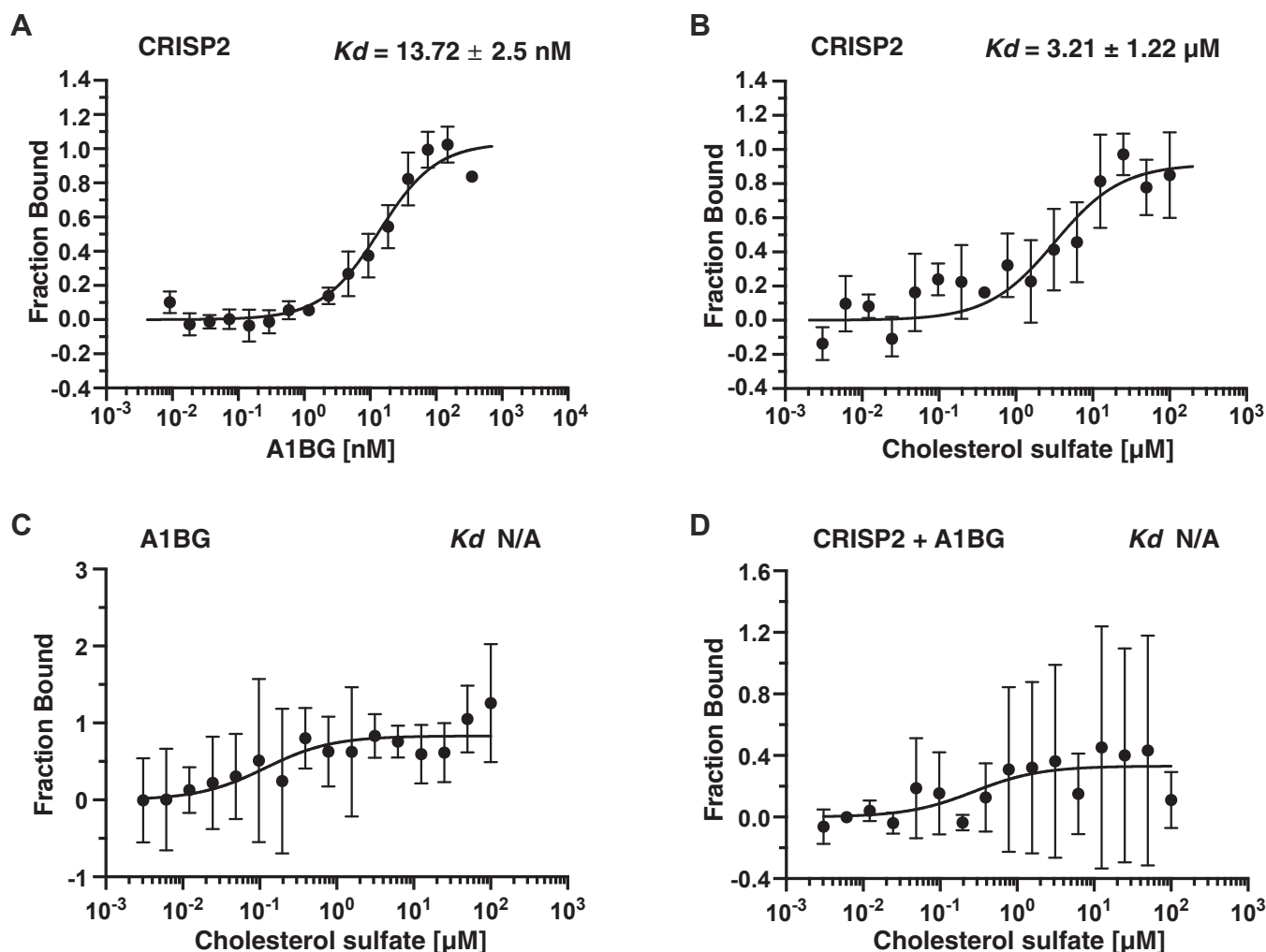


**Figure 2. A1BG binds CRISP2 *in vitro* and blocks sterol binding.** A, the direct interaction between A1BG and CRISP2 was assessed by MST. Purified and fluorescently labeled CRISP2 protein was incubated with increasing concentrations of unlabeled A1BG and complex formation was analyzed. MST measurements were performed in triplicates, and the corresponding dissociation constant ( $K_d$ ) is indicated. B–D, sterol-binding by CRISP2 in the absence (panel B) or the presence of A1BG (panel D) was assessed by MST. CRISP2 binds cholesterol sulfate in the low micromolar range, but this binding is blocked in the presence of A1BG, which by itself does not bind cholesterol sulfate (panel C). Measurements were performed in triplicates and the corresponding dissociation constants ( $K_d$ ) are indicated. N/A; not applicable. A1BG, alpha-1-B glycoprotein; CRISP, cysteine-rich secretory protein; MST, microscale thermophoresis.

individually in yeast and tested its ability to inhibit the Pry1- and CRISP2-mediated export of cholesterol. This systematic approach revealed that expression of the Ig3 domain of A1BG significantly reduced the export of cholesterol mediated by both tested CAP proteins (Fig. 4, A and B). The fact that the Ig3 domain of A1BG inhibits cholesterol export of both Pry1 and CRISP2 indicates that the mode of interaction between Ig3 and the CAP domain is conserved. Analysis of the synthesis and secretion of Pry1 and CRISP2 in cells expressing individual Ig domains of A1BG by Western blotting indicated that both CAP family proteins were expressed and secreted, as were the five different Ig domains of A1BG (Fig. 4C).

To validate these *in vivo* results, we expressed three individual Ig domains of A1BG, Ig1, Ig3, and Ig4 in *Escherichia coli* and purified hexahistidine-tagged versions of these domains. The binding affinities of these Ig domains to CRISP2 were then assessed by MST. Ig1 and Ig3 were

chosen as they are both predicted to interact strongly with CRISP2, while Ig4 was used as a negative control that is neither predicted to interact with CRISP2 nor affect its sterol binding function (Figs. 3D and 4B). Consistent with the predictions from the *in silico* docking analysis, MST measurements revealed a high affinity interaction between Ig3 and CRISP2 ( $K_d$   $13.8 \pm 1.14$  nM) and a weaker interaction with Ig1 ( $K_d$   $38.7 \pm 38.4$  nM), but no detectable interaction with Ig4 (Fig. 5A). These interactions between individual Ig domains of A1BG and CRISP2 were confirmed by immunoprecipitation of protein complexes present in the culture supernatant of cells expressing tagged versions of these proteins (Fig. 5B). Quantification of these results indicated that immunoprecipitation of the HA-tagged versions of CRISP2 resulted in a significant coprecipitation of FLAG-tagged Ig3, whereas signals of Ig1 and Ig4 remained at much lower levels (Fig. 5C). Taken together, these results indicate that the interaction between the Ig3 domain of

A1BG inhibits sterol-binding by CRISP2

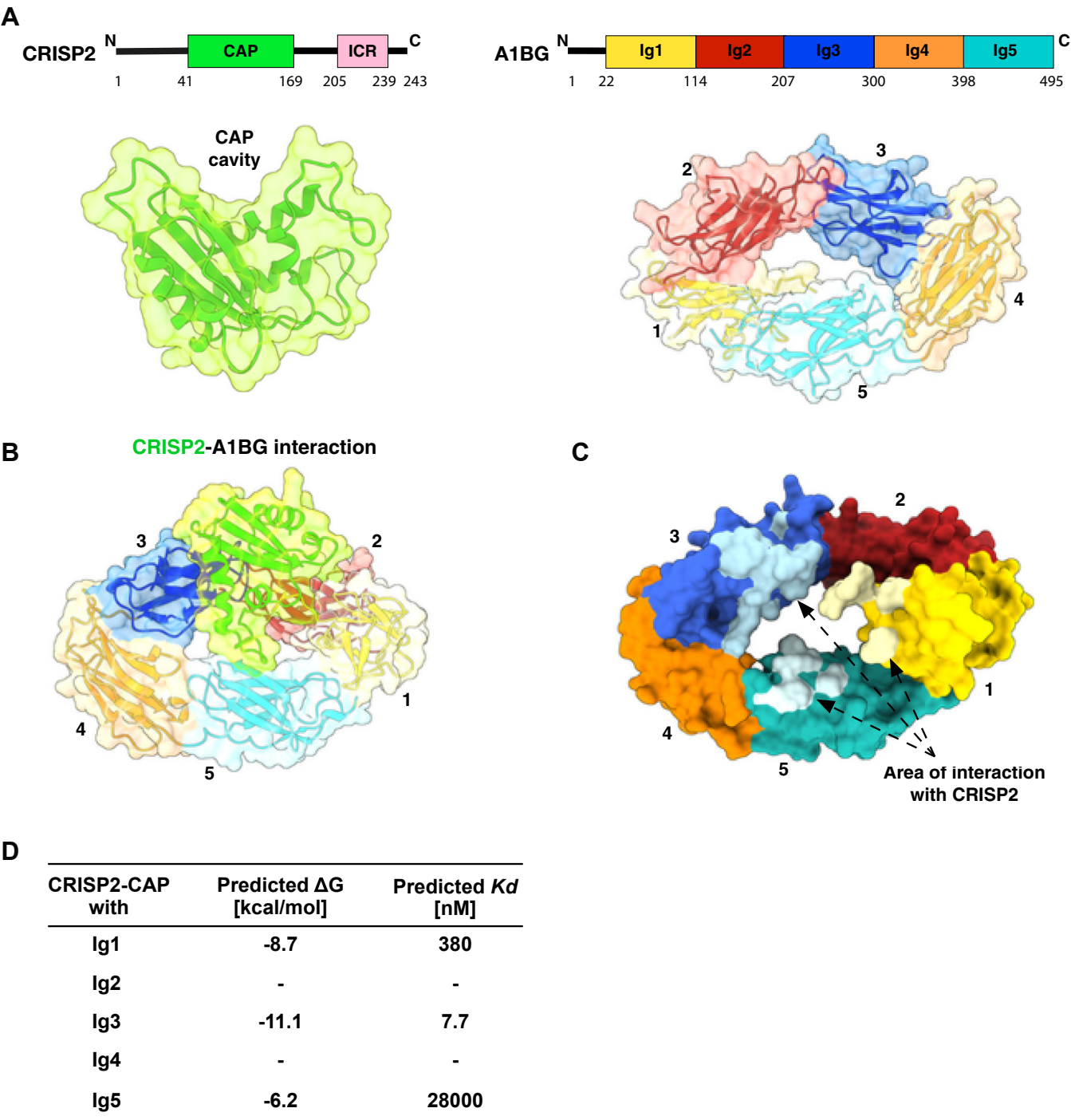


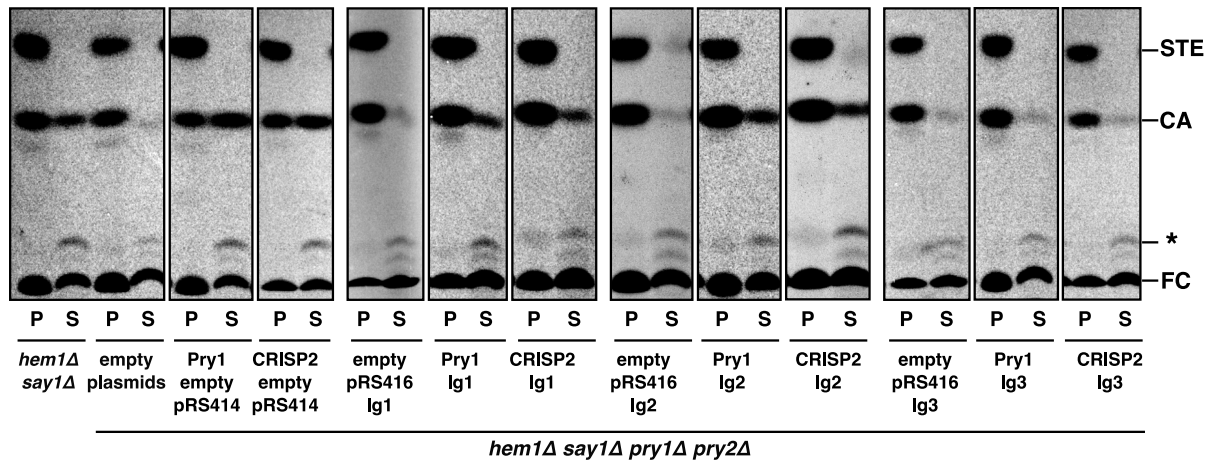
**Figure 3. *In silico* docking of CRISP2 to A1BG.** A, schematic representation of CRISP2 and A1BG. The CAP domain (green box) and the ion channel regulatory domain (ICR, pink box) of CRISP2 are depicted. The five immunoglobulin (Ig) domains of A1BG are color coded. Amino acid positions of domain boundaries are indicated. The structures of both proteins as predicted by AlphaFold2 are shown below in a combined ribbon/surface representation. The large CAP cavity within the CAP domain of CRISP2 is indicated as is the ring-shaped alignment of the five Ig domains of A1BG. B, the predicted interaction of the CAP domain of CRISP2 (green) with A1BG is shown using a combined ribbon/surface representation. C, the area of surface-to-surface interaction between the CAP domain of CRISP2 and the individual Ig domains of A1BG are indicated in light colors. The largest surface interaction occurs between the Ig3 domain of A1BG and the CAP domain of CRISP2, followed by that of Ig1 and Ig5. D, table depicting the predicted interaction between CRISP2 and individual Ig domains of A1BG. Free energy ( $\Delta G$ ) and affinities ( $K_d$ ) of interactions between CRISP2 and individual Ig domains of A1BG as predicted by PRODIGY are listed. A1BG, alpha-1-B glycoprotein; CRISP, cysteine-rich secretory protein; PRODIGY, PROtein binDing enerGY prediction.

A1BG and CRISP2 is of high affinity and can be detected both by MST analysis of purified components *in vitro* and in the supernatant of cells expressing tagged versions of these proteins.

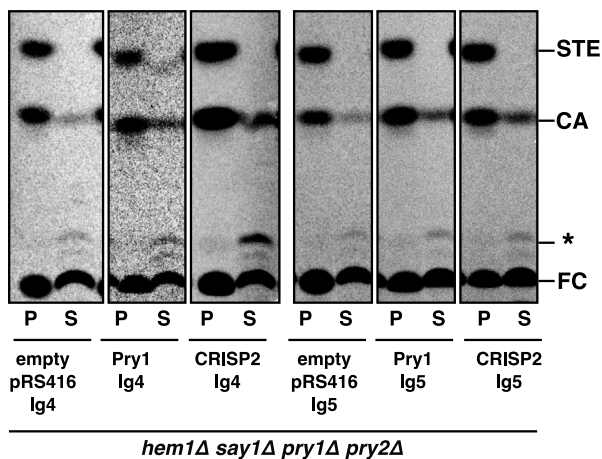
**The Ig3 repeat domain of A1BG inhibits cholesterol binding by CRISP2 *in vitro***

Given that the Ig3 domain of A1BG is sufficient for high affinity interaction with CRISP2, we next tested whether Ig3

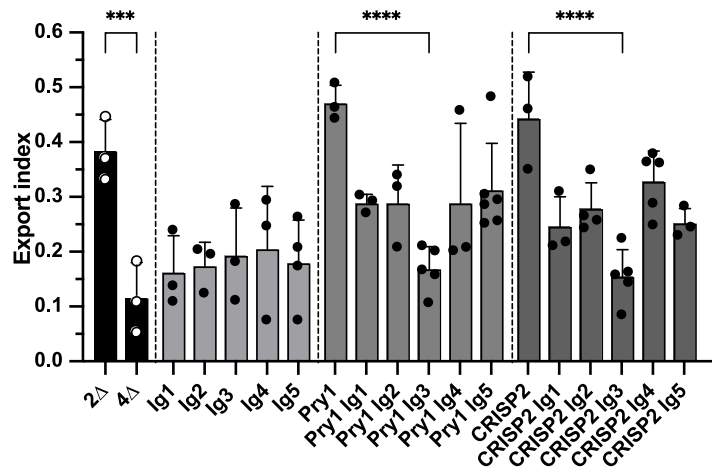
A



A (continue)



B



C

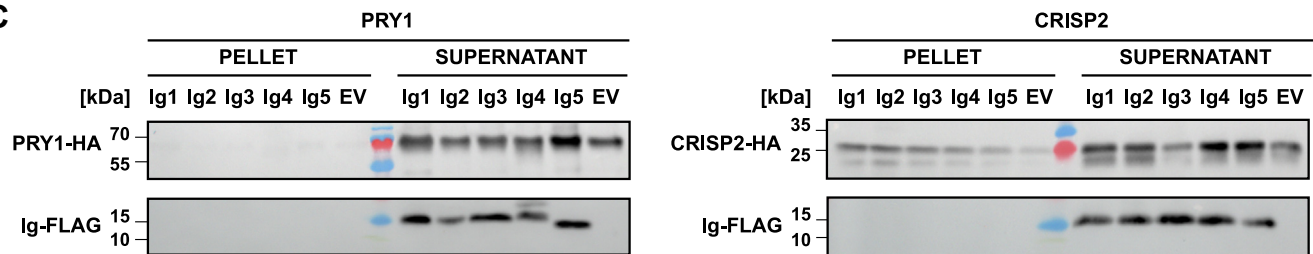


**Figure 4. Expression of the Ig3 domain of A1BG inhibits cholesterol export by Pry1 or CRISP2.** A, sterol export by yeast Pry1 and mammalian CRISP2 in the presence of the five different Ig domains, Ig1-Ig5, of A1BG. Quadruple mutant cells (*hem1Δ say1Δ pry1Δ pry2Δ*) expressing different combination of either empty plasmids (pRS414, pRS416), plasmids containing the indicated Ig domains of A1BG, or plasmids for the expression of the CAP proteins Pry1 and CRISP2 were labeled with [ $^{14}$ C]-cholesterol. Lipids were extracted from both the cell pellet (P) and the culture supernatant (S), separated by TLC, and visualized by phosphorimaging. The position of free cholesterol (FC), cholesterol acetate (CA), sterol esters (STE), and an unidentified lipid (\*) are indicated to the right. B, export of radiolabeled cholesterol acetate is plotted as export index in the graph. Data correspond to means  $\pm$  S.D. of three independent determinations and statistical significance is indicated: \*\*\* $p \leq 0.001$ ; \*\*\*\* $p \leq 0.0001$  (one-way ANOVA with Tukey's *post hoc* test). C, expression of the Ig domains of A1BG does not block the synthesis or secretion of the CAP family members Pry1 or CRISP2. Proteins were TCA precipitated from the cell pellet (P) or the culture supernatant (S) of cells expressing HA-tagged Pry1 or CRISP2, in the absence (pRS414, empty plasmid) or the presence of FLAG-tagged Ig domains of A1BG and analyzed by Western blotting. A1BG, alpha-1-B glycoprotein; CRISP, cysteine-rich secretory protein; HA, hemagglutinin; Ig, immunoglobulin; TCA, trichloroacetic acid.

alone could also inhibit the binding of cholesterol by CRISP2 *in vitro* (Fig. 6A). MST analysis indicated that the presence of Ig3, but not that of Ig1 or Ig4, was indeed sufficient to block binding of cholesterol by CRISP2 (Fig. 6, B–D). Control

experiments indicated that none of the Ig domains alone could bind cholesterol (Fig. 6, E–G). These data indicate that binding of the Ig3 domain of A1BG to CRISP2 is sufficient to inhibit the cholesterol binding by CRISP2 *in vitro*.

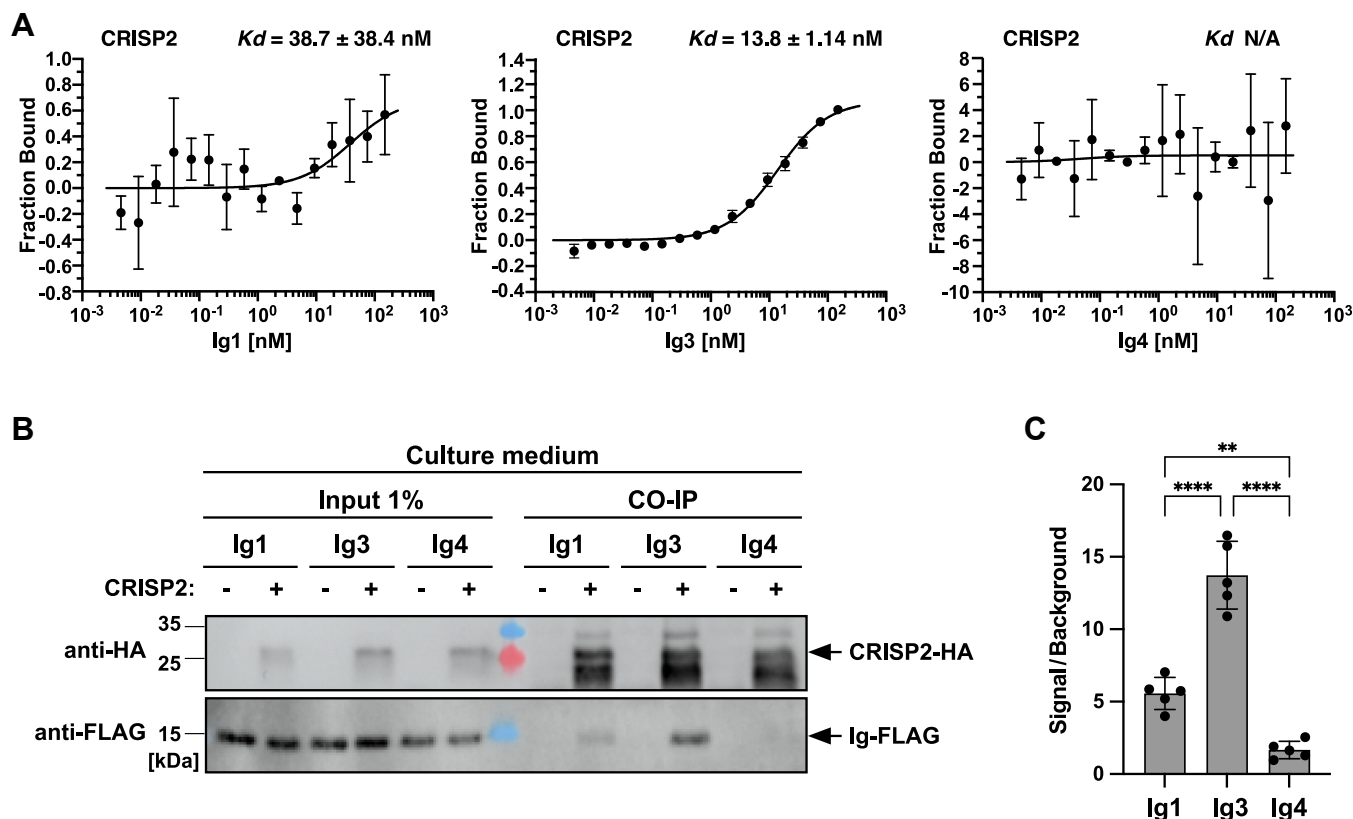


**Figure 5. The Ig3 domain of A1BG displays high affinity interaction with CRISP2 *in vitro* and *in vivo*.** A, the *in vitro* interaction between three different Ig domains of A1BG, Ig1, Ig3, and Ig4 and CRISP2 was assessed by microscale thermophoresis. Purified and fluorescently labeled CRISP2 protein was incubated with increasing concentrations of unlabeled purified Ig domains of A1BG, Ig1, Ig3, and Ig4, and complex formation was analyzed. Measurements were performed in triplicates and the corresponding dissociation constant ( $K_d$ ) is indicated. N/A; not applicable. B, the *in vivo* interaction between three different Ig domains of A1BG, Ig1, Ig3, and Ig4 and CRISP2 was assessed by co-immunoprecipitation. Cells expressing FLAG-tagged Ig domains of A1BG, Ig1, Ig3, or Ig4 (a) and cells coexpressing FLAG-tagged Ig domains together with HA-tagged CRISP2 (b) were cultivated, and the interaction between the Ig domains of A1BG and CRISP2 in the culture medium was analyzed by immunoprecipitation with an anti-HA antibody followed by Western blotting to detect both HA-tagged CRISP2 and FLAG-tagged Ig domains. C, quantification of the interaction between the Ig domains of A1BG and CRISP2. The interaction between Ig1, Ig3, or Ig4 and CRISP2 detected by Co-IP were quantified and plotted as ratio between the signal obtained from cells expressing both proteins, CRISP2-HA and Ig-FLAG (+), divided by the background signal from cells lacking CRISP2-HA (–). Data represent mean  $\pm$  S.D. of 5 determinations and statistical significance is indicated:  $^{**}p \leq 0.01$ ;  $^{****}p \leq 0.0001$  (one-way ANOVA with Tukey's *post hoc* test). A1BG, alpha-1-B glycoprotein; CRISP, cysteine-rich secretory protein; HA, hemagglutinin.

### A mutant version of CRISP2, CRISP2<sup>L98G Y99P</sup>, affects the interaction with A1BG

To characterize the molecular basis of the binding between CRISP2 and A1BG in more detail, we aimed to identify residues of the two proteins that are important for stabilizing their interaction. A more detailed analysis of the *in silico* predicted interaction between the two proteins indicated that their interaction occurs primarily through an antiparallel  $\beta$ -sheet formed between CRISP2 and A1BG (Fig. 7A). A similar type of interaction was previously observed between CRISP2 and prostate secretory protein of 94 amino acids (PSP94), a major protein component in the seminal plasma (35). To test the functional importance of residues within the second  $\beta$ 2-strand of CRISP2, we tested whether mutations in two key residues within this structure, namely the leucine residue at position 98 (L98) and the following tyrosine residue (Y99), would affect the interaction between CRISP2 and A1BG. A CRISP2<sup>L98G Y99P</sup> point mutant version still interacted with the Ig3 domain of A1BG, albeit at lower affinity ( $K_d$  21.0  $\pm$  4.1 nM) than did the WT protein ( $K_d$  13.8  $\pm$  1.14 nM) (Figs 5A and 7B). As reported

before, the CRISP2<sup>L98G Y99P</sup> point mutant version still bound cholesterol with high affinity ( $K_d$  0.18  $\pm$  0.06  $\mu$ M), but sterol binding was inhibited in the presence of the Ig3 domain of A1BG (Fig. 7C). Additionally, when tested for cholesterol export in the *in vivo* assay, the Ig3 domain of A1BG still inhibited secretion of cholesterol by the CRISP2<sup>L98G Y99P</sup> mutant version (Fig. 7, D and E). These results suggest that the mutation of these two interfacial residues does not strongly affect the function of Ig3 to inhibit sterol binding by CRISP2 *in vivo*. The CRISP2<sup>L98G Y99P</sup> point mutant was synthesized and secreted comparable to the WT CRISP2 protein, suggesting that the mutations do not affect the overall folding or stability of the protein (Fig. 7F).

### The interaction between CRISP2 and the Ig3 domain of A1BG is dependent on magnesium ions

CAP family proteins have highly conserved tetrad residues with which they can coordinate divalent cations such as  $Mg^{2+}$  or  $Zn^{2+}$ . This cation-coordination is important for the function of these proteins in different physiological settings,

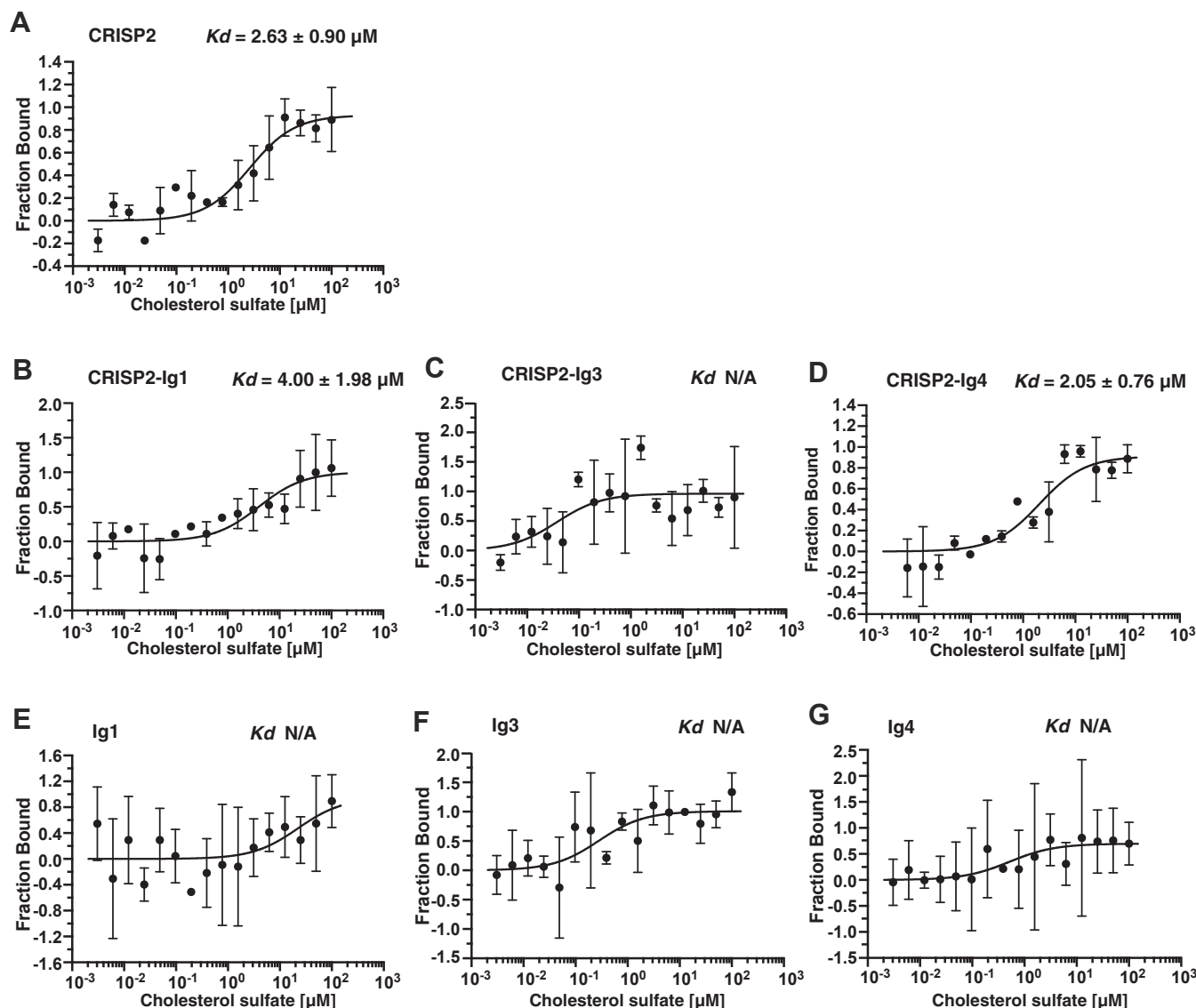


**Figure 6. The Ig3 domain of A1BG blocks sterol binding by CRISP2 *in vitro*.** A–D, sterol-binding by CRISP2 in the absence (panel A) or the presence of purified Ig domains of A1BG (panels B–D) was assessed by microscale thermophoresis. CRISP2 bound cholesterol sulfate in the low micromolar range (panel A). Sterol binding by CRISP2 is not affected in the presence of the Ig1 (panel B) or Ig4 (panel D) domains of A1BG but is blocked in the presence of Ig3 (panel C). E–G, the Ig domains by themselves do not bind cholesterol. Measurements were performed in triplicates and the corresponding dissociation constants ( $K_d$ ) are indicated. N/A; not applicable. A1BG, alpha-1-B glycoprotein; CRISP, cysteine-rich secretory protein; Ig, immunoglobulin.

including their ability to bind sterols or to inhibit the yeast mating reaction (Fig. 8A) (5–8, 48). To test whether coordination of divalent cations is crucial for the interaction between CRISP2 and the Ig3 domain of A1BG, we tested their interaction in the presence of the magnesium chelator EDTA. Addition of 5 mM EDTA to the MST binding buffer essentially abrogated the interaction between CRISP2 and the Ig3 domain of A1BG (Fig. 8B). Protein binding could be restored by the addition of  $\text{MgCl}_2$ , thus confirming the cation-dependence of the interaction (Fig. 8B). Addition of  $\text{ZnCl}_2$ , on the other hand, failed to restore protein binding, indicating that  $\text{Mg}^{2+}$  is the preferred cation over  $\text{Zn}^{2+}$  (Fig. 8B). This magnesium-dependence of the protein interaction was not only observed with the single Ig3 domain of A1BG but also with full-length A1BG protein

(Fig. 8C). Lastly, we examined whether cholesterol binding by CRISP2 is dependent on the presence of divalent cations. In the presence of EDTA, CRISP2 failed to bind cholesterol in a dose-dependent manner (Fig. 8D). Cholesterol binding could be reconstituted by the back-addition of  $\text{Mg}^{2+}$  but not by the addition of  $\text{Zn}^{2+}$ , indicating that  $\text{Mg}^{2+}$  might be the preferred cation for coordination of the highly conserved tetrad residues, which is consistent with the presence of  $\text{Mg}^{2+}$  in the crystal structure of the CAP domain of yeast Pry1 (Fig. 8A) (8). Taken together, these data indicate that CRISP2 interacts with A1BG, particularly through the Ig3 domain of A1BG, and that this interaction depends on the coordination of  $\text{Mg}^{2+}$  through the highly conserved tetrad residues within the CAP domain of CRISP2.

# A1BG inhibits sterol-binding by CRISP2

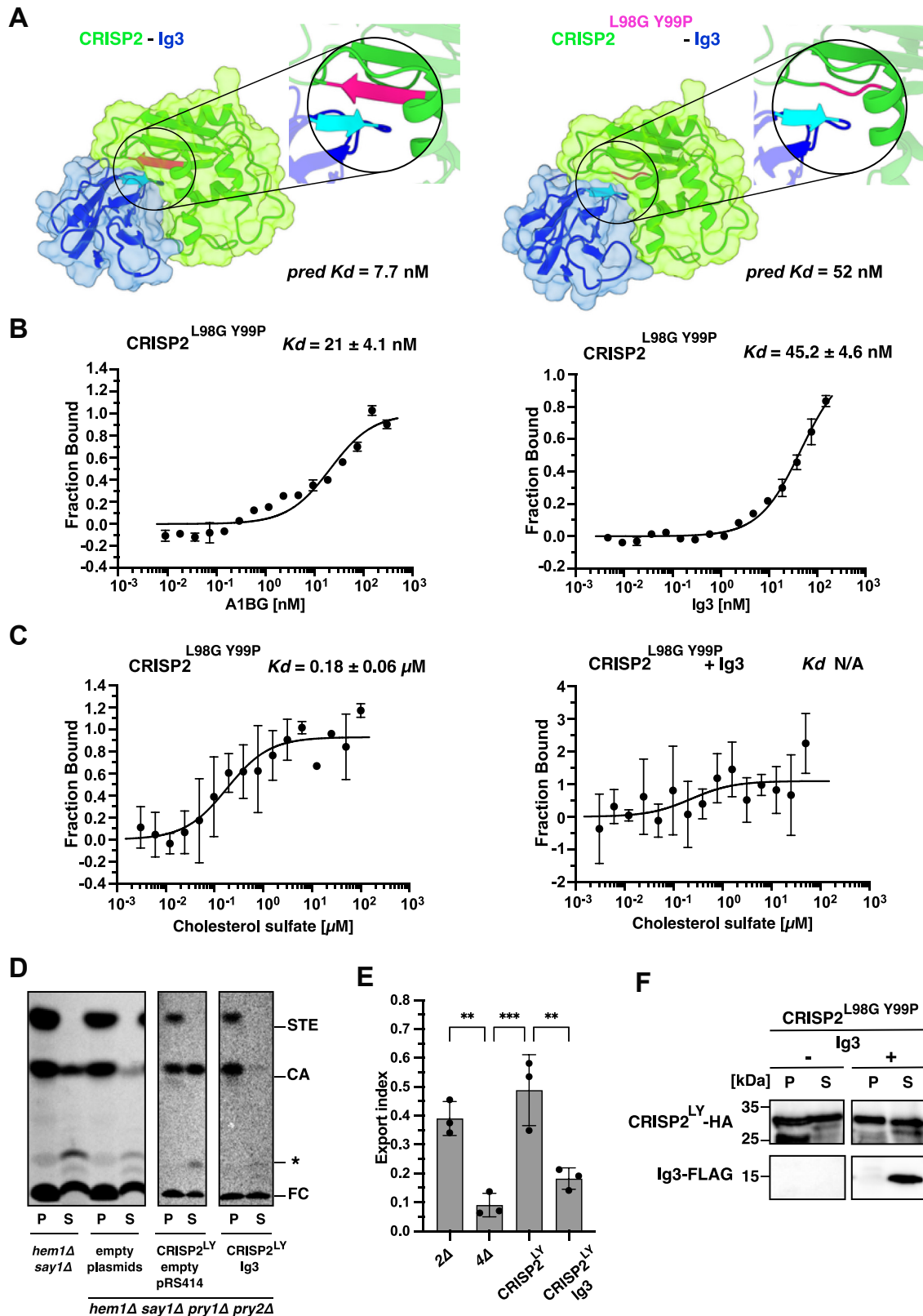


**Figure 7. The interaction between the Ig3 domain of A1BG and CRISP2 is affected by mutations in the  $\beta$ 2-strand of CRISP2.** *A*, Model of the interaction between the Ig3 domain of A1BG and CRISP2. The interaction between the Ig3 domain (blue) and CRISP2 (green) as predicted by *in silico* docking using AlphaFold. The complex between Ig3 and CRISP2 is mainly stabilized by the interaction between a  $\beta$ -sheet of Ig3 (highlighted in light blue) and the antiparallel  $\beta$ 2-strand of CRISP2 (pink) involving the stabilizing residues L98 and Y99. Mutations of both L98 and Y98 to glycine and proline are predicted to disturb the  $\beta$ 2-strand of CRISP2 (right-hand panel) resulting in a decreased affinity between Ig3 and CRISP2 as indicated by the dissociation constant predicted by PRODIGY (*pred K<sub>d</sub>*). *B* and *C*, mutations within the  $\beta$ 2-strand residues L98 and Y99 of CRISP2 affect its interaction with A1BG and Ig3. The binding of the CRISP2<sup>L98G Y99P</sup> double mutant version with A1BG, the Ig3 domain, and cholesterol sulfate was assessed by MST. The presence of Ig3 still inhibited sterol binding by CRISP2<sup>L98G Y99P</sup>. Measurements were performed in triplicates and the corresponding dissociation constants (*K<sub>d</sub>*) are indicated. N/

## Discussion

Here, we focus on the interaction between the mammalian CAP superfamily member CRISP2 and the serum glycoprotein A1BG. A1BG binds CRISP2 and thereby impedes sterol-binding by CRISP2 both *in vivo* and *in vitro*. The nanomolar binding affinity observed between A1BG and CRISP2 ( $K_d$  13.7 nM) indicates a strong and biologically relevant interaction. Such affinities are typically observed in regulatory protein interactions, underscoring the potential physiological importance of this binding in modulating sterol-binding functions. A1BG is composed of five repeated Ig domain, and *in silico* docking predicted strong interactions between A1BG and CRISP2, particularly through the Ig3 domain of A1BG. This finding was validated experimentally, showing that Ig3 alone could inhibit CRISP2-mediated sterol-binding, reinforcing the structural significance of the Ig3 domain in this interaction. Ig3 interacts with CRISP2 through the formation of an intermolecular antiparallel  $\beta$ -sheet, as mutations in conserved amino acids within the  $\beta$ 2-strand of CRISP2 decrease binding of A1BG and that of the Ig3 domain of A1BG to CRISP2. We finally show that  $Mg^{2+}$ -coordination, most likely through the highly conserved tetrad residues within the CAP domain of CRISP2 is required for high affinity interaction with A1BG or the Ig3 domain of A1BG. Interestingly,  $Zn^{2+}$  which has also been reported as a divalent cation coordinated by these CAP domain residues does not substitute for the requirement of  $Mg^{2+}$  in promoting binding of A1BG or that of cholesterol sulfate to CRISP2 (5–8).

A1BG is a low abundant serum glycoprotein of unknown function that has been associated with several pathologic conditions (20). A1BG contains five repeated Ig folds, this fold is structurally very stable and shows remarkable plasticity in terms of its binding specificity (21–23). Proteins that use this fold perform many functions related to immunological recognition and they also associate with several developmental and homeostatic processes (23, 49). Interestingly, the formation of high-affinity heteromeric complexes between small Ig fold-containing secreted proteins appears to be an evolutionarily conserved mechanism to inhibit target protein function. For example, A1BG-like plasma proteins from opossum species form complexes with toxins from reptiles, including snake venom, suggesting a role in neutralizing venom toxicity (50–53). Oprin, for example, an opossum inhibitor of snake venom metalloproteinases shows high similarity (36% identity) with human A1BG and contains four of the five Ig repeat domains found in A1BG. The presence of oprin in opossum serum may partially account for the resistance of this marsupial to localized effects of rattlesnake

envenomation, caused by venom metalloproteinases (50). It is interesting to note that almost all of the known venom toxin inhibitor proteins are associated with the Ig supergene family; for this reason, it has been suggested that these proteins are a derived part of the innate immune system (54–56). While there are no detectable A1BG homologs in the yeast genome, or reported interactors that might mimic the function of A1BG, we think that the heterologous yeast system can serve as an attractive tool to study the possible physiological consequences of CAP family members and their interactors (3, 10, 57).

Thus, remarkably, two human serum proteins PSP94 and A1BG, both of which show high affinity binding to CRISP have homologs in other species, which function to neutralize the toxicity of CRISP family members from venomous snakes (18, 35, 54, 58). CRISP family proteins from snake venoms exert their neurotoxic function by inhibiting ion channels, through their C terminal cysteine-rich domain (18, 59, 60). Their autotoxicity is efficiently neutralized by binding to an endogenous protein, which belongs to the PSP94 family of proteins (35, 61). Given that complex formation between the Ig repeat containing oprin and related proteins inhibits snake venom toxins and thereby protects the animal from envenomation, complex formation between A1BG and CRISP3 has also been proposed to exert a similar function in mammals by protecting the circulation from a potentially harmful effect of free CRISP3 (32, 62).

Taken together, our results highlight a novel inhibitory mechanism by which A1BG regulates the sterol-binding function of CRISP2. This interaction may be evolutionarily conserved, with broader implications in immune defense and cancer biology (63, 64). Further studies should explore the physiological relevance of this interaction in cancer cells and its potential as a therapeutic target.

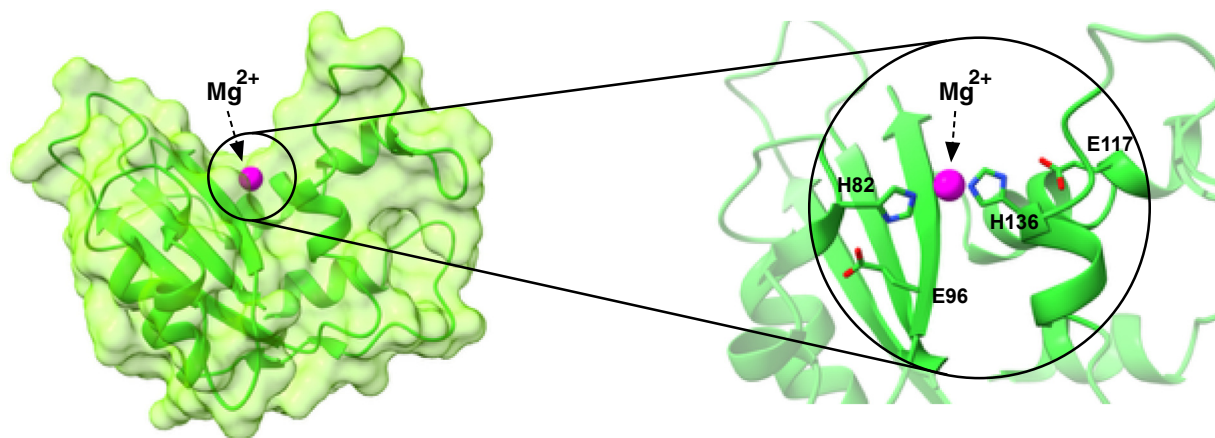
## Experimental procedures

### S. cerevisiae strains, growth conditions, and plasmids

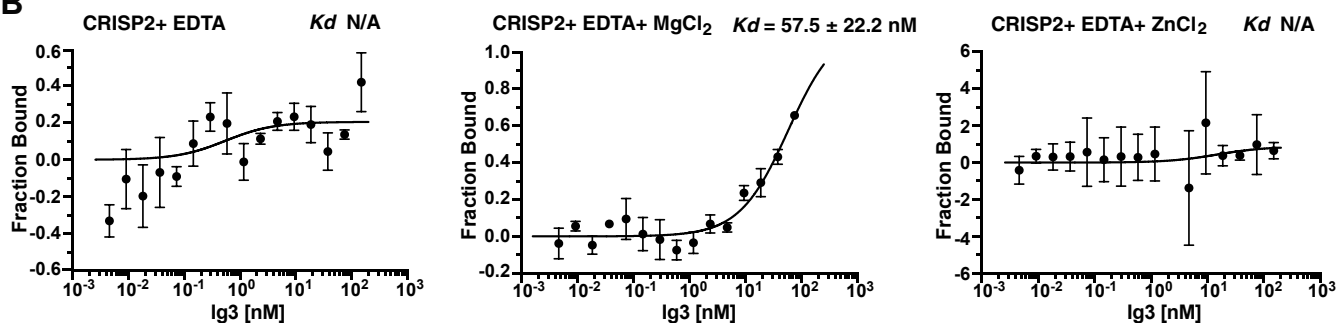
*S. cerevisiae* double mutant *say1 $\Delta$  hem1 $\Delta$*  (2 $\Delta$ ) and quadruple mutant *say1 $\Delta$  hem1 $\Delta$  pry1 $\Delta$  pry2 $\Delta$*  (4 $\Delta$ ) strains were generated using PCR deletion cassettes and marker rescue strategies (Table S2). Double mutant strains were grown in yeast peptone dextrose media whereas quadruple mutants were grown in synthetic complete (SC) media. To compensate for the heme deficiency, cells were cultivated either in medium supplemented with delta-aminolevulinic acid (10  $\mu$ g/ml), or in medium containing cholesterol (20  $\mu$ g/ml) and Tween-80 (0.05 mg/ml).

A; not applicable. D, export of cholesterol by the CRISP2<sup>L98G Y99P</sup> mutant version is impaired in the presence of Ig3. Quadruple mutant cells (*hem1 $\Delta$  say1 $\Delta$  pry1 $\Delta$  pry2 $\Delta$* ) expressing CRISP2<sup>L98G Y99P</sup> and carrying either an empty plasmid (pRS414) or a plasmid containing the Ig3 domains of A1BG were labeled with [<sup>14</sup>C]-cholesterol. Lipids were extracted from both the cell pellet (P) and the culture supernatant (S), separated by TLC, and visualized by phosphorimaging. The position of free cholesterol (FC), cholesterol acetate (CA), steryl esters (STE), and an unidentified lipid (\*) are indicated to the right. E, quantification of export of radiolabeled cholesterol acetate is plotted as export index. Data correspond to means  $\pm$  S.D. of three independent determinations and statistical significance is indicated: \*\* $p \leq 0.01$ ; \*\*\* $p \leq 0.001$  (one-way ANOVA with Tukey's *post hoc* test). F, expression of the Ig3 domains of A1BG does not affect the synthesis or secretion of the CRISP2<sup>L98G Y99P</sup> mutant version in yeast. Proteins were TCA precipitated from either the cell pellet (P) or the culture supernatant (S) of cells expressing HA-tagged CRISP2<sup>L98G Y99P</sup>, in the absence (pRS414, empty plasmid) or the presence of a FLAG-tagged Ig3 domain and analyzed by Western blotting. A1BG, alpha-1-B glycoprotein; CRISP, cysteine-rich secretory protein; Ig, immunoglobulin; HA, hemagglutinin; L98, leucine residue at position 98; MST, microscale thermophoresis; PRODIGY, PROtein binDing energy prediction; TCA, trichloroacetic acid.

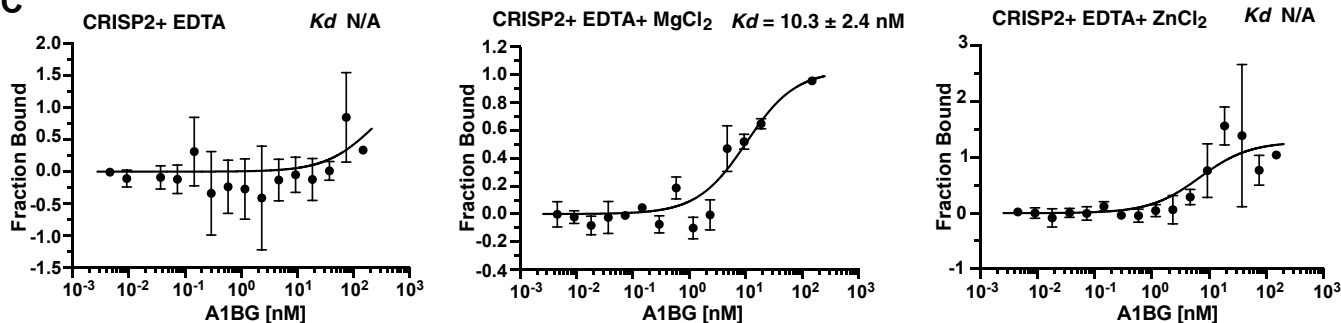
A



B



C



D

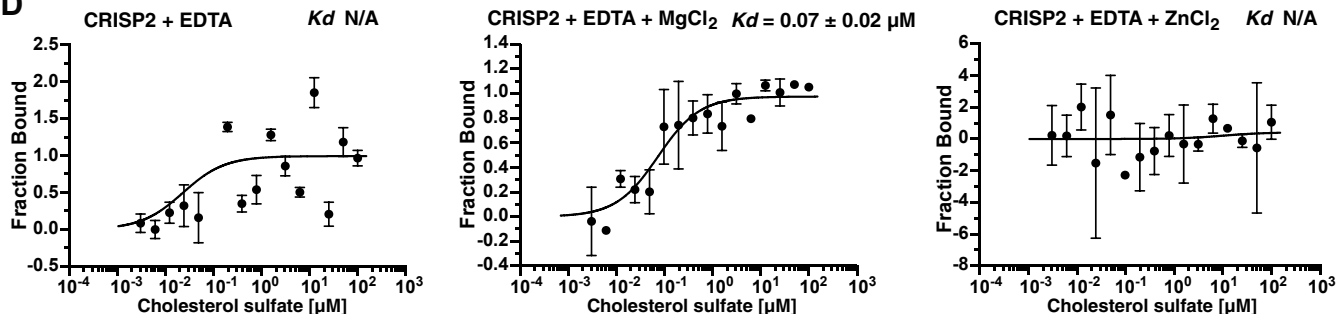


**Figure 8. CRISP2 requires magnesium for binding of Ig3, A1BG, or cholesterol.** A, model of the CAP domain of CRISP2 showing the highly conserved tetrad residues proposed to coordinate binding of divalent cations.  $Mg^{2+}$  is indicated in *magenta*, the conserved tetrad residues (H82, E96, E117, and H136) are indicated. B and C, binding of the Ig3 (panel B) domain of A1BG or that of full-length A1BG (panel C) by CRISP2 is dependent on magnesium. Binding of Ig3 or A1BG by CRISP2 was assessed by MST in the presence of EDTA (5 mM), EDTA and  $MgCl_2$  (10 mM), or EDTA and  $ZnCl_2$  (20 mM). D, binding of cholesterol sulfate by CRISP2 requires magnesium. Binding of cholesterol sulfate by CRISP2 was assessed by MST in the presence of EDTA,  $MgCl_2$  or  $ZnCl_2$ . All MST measurements were performed in triplicates and the corresponding dissociation constants ( $K_d$ ) are indicated. N/A; not applicable. A1BG, alpha-1-B glycoprotein; CRISP, cysteine-rich secretory protein; Ig, immunoglobulin; MST, microscale thermophoresis.

Plasmids encoding for CAP proteins were constructed by cloning of PCR amplified fragments from *S. cerevisiae* genomic DNA or from codon optimized synthesized genes (GenScript) into plasmid pRS416, containing an *URA3* selection marker (Table S3). Genes were expressed from an *ADHI* promoter and fused to the signal sequence of pre-pro alpha factor. Codon optimized A1BG and its domains were cloned into pRS414 using hygromycin as selection marker. A1BG full length and its Ig domains were expressed from an *ADHI* promoter and fused either to the signal sequence of Pry1 or that of pre-pro alpha factor.

### In vivo sterol export assay

The sterol export assay was performed as described (38). *S. cerevisiae* mutants deficient in heme biosynthesis (*hem1Δ*), lacking the sterol deacetylase enzyme Say1 (*say1Δ*), Pry1 (*pry1Δ*), and Pry2 (*pry2Δ*), were grown overnight in the presence of cold cholesterol/Tween-80. For strains containing pRS414, 80 μg/ml hygromycin was added to the medium. On the second day, cells were harvested by centrifugation, washed twice with SC medium, and then diluted to  $A_{600\text{nm}}$  of 1 into fresh medium containing 0.025 μCi/ml [ $^{14}\text{C}$ ]-cholesterol. After overnight growth, cells were washed again with SC medium and cultivated for another day with nonradiolabeled cholesterol containing media. Cells were then centrifuged, and lipids were extracted from both the cell pellet and the culture supernatant using chloroform/methanol (1:1, v/v). Extracted radiolabeled lipids were quantified by scintillation counting, and volumes corresponding to 10,000 cpm (counts per minute) were dried. Dried lipids were resuspended in chloroform/methanol and separated by TLC on silica gel 60 plates (Merck) using the solvent system petroleum ether/diethyl ether/acetic acid (70:30:2, v/v/v). TLC plates were then exposed to phosphorimager screens, and radiolabeled lipids were visualized and quantified using a phosphorimager (GE HealthCare). The sterol export index was calculated as the ratio of extracellular CA to the sum of intracellular and extracellular CA. Export experiments were performed in triplicate, and the export index is given as mean  $\pm$  SD of three independent experiments. Statistical analysis was performed with one way ANOVA, using Prism (GraphPad Software; <https://www.graphpad.com/>).

### Fatty acid export

To analyze the CRISP2-dependent export of fatty acids in the presence or absence of A1BG, cells (*faa1Δ faa4Δ pry1Δ pry3Δ*) were grown overnight, the supernatant of 3  $A_{600\text{nm}}$  units of yeast cells was collected, and lipids were extracted in chloroform:methanol:HCl (50:100:1.5; v/v/v), supplemented with an internal standard (C17:0). The organic phase was collected and dried under a stream of nitrogen. Fatty acid methyl esters (FAMES) were produced by incubating the dried fractions at 85 °C for 45 min in 1 ml of methanol-sulfuric acid (5% v/v) supplemented with butylated hydroxytoluene (0.01% w/v). The FAMES were extracted in a mixture containing 1.5 ml of NaCl (0.9% w/v) and 2 ml of hexane, and the upper phase was collected. FAMES were then resuspended in hexane and

separated on an Agilent 7890A gas chromatograph (GC) equipped with a DB-23 capillary column (30 m  $\times$  0.25 mm  $\times$  0.25 μm) (Agilent Technologies) and quantified relative to an internal standard (C17:0, 10 μg) as described before (44, 46).

### Protein secretion analysis and Western blotting

To analyze the expression and secretion of CAP proteins, they were tagged with a HA tag (YPYDVPDYA) and A1BG or its Ig domains were tagged with a FLAG tag (DYKDDDDK). Epitope-tagged proteins were extracted from 3  $A_{600\text{nm}}$  units of cells with 0.185 M NaOH (65), followed by precipitation with 10% TCA. To analyze their secretion into the culture supernatant, total proteins from 20 ml culture medium was precipitated with 10% TCA, acetone washed, solubilized in sample buffer, and analyzed by SDS-PAGE and Western blotting. Western blotting was performed using rat anti-HA antibody (rat, 1:2000, Roche #11867423001), and FLAG monoclonal antibody (mouse, 1:2000, Sigma-Aldrich #F3165). As secondary antibodies: goat anti-rat IgG antibody, horseradish peroxidase conjugate (1:10,000, Merck #AP136P) and goat anti-mouse IgG (horseradish peroxidase) conjugates (1:10,000, Bio-Rad #1706516) were used. ECL Prime chemiluminescence substrate (Sigma-Aldrich) was used for signal development and chemiluminescence was detected with an ImageQuant LAS 4000 biomolecular imager (GE HealthCare; <https://www.cytivalifesciences.com>). Experiments were performed in triplicates with similar results.

### Protein expression and purification

DNA encoding proteins of interest were PCR amplified and cloned into NcoI and XhoI restriction sites of pET22b, which contains a PelB signal sequence to direct the secretion of expressed protein into the periplasmic space. Plasmids were transformed into *E. coli* BL21, and proteins were expressed with a C-terminal polyhistidine-tag. Different induction strategies were used: overnight induction with lactose at 24 °C for CRISP2 and A1BG, and 6 h of induction with 0.4 mM IPTG at 24 °C for the Ig1 and Ig4 domains of A1BG, and at 30 °C for Ig3. Cells were collected, lysed, and the soluble cell lysates were incubated with nickel-nitrilotriacetic acid beads as per the manufacturer instructions (Qiagen). Beads were washed, loaded onto a column, and proteins were eluted with a buffer containing 60 mM  $\text{NaH}_2\text{PO}_4$ , 300 mM NaCl, and 300 mM imidazole, pH 8.0. For MST experiments, proteins were applied to Zeba desalting spin columns (Thermo Fisher Scientific), and the buffer was exchanged to 60 mM  $\text{NaH}_2\text{PO}_4$ , 300 mM NaCl, pH 8.0. Protein concentration was determined by Lowry assay using the Folin reagent and bovine serum albumin as a protein standard.

### Microscale thermophoresis

To assess protein-protein and protein-lipid interactions, MST experiments were performed using a Monolith NT.115 (Nanotemper Technologies). Proteins were labeled using the RED-tris-NTA His tag protein labeling kit. Subsequently,

## A1BG inhibits sterol-binding by CRISP2

100 nM of labeled CRISP2 protein or the L98G Y99P mutant version of CRISP2 were mixed with a serial dilution of unlabeled A1BG, the Ig domains of A1BG, cholesterol sulfate, or palmitic acid, prepared in binding buffer (20 mM Tris pH 7.5, 30 mM NaCl, and 0.05% Triton X-100). Samples were loaded into MST standard capillaries, and MST measurements were performed using an 80% laser power setting. The dissociation constant  $K_d$  was obtained by plotting the fraction bound against the logarithm of ligand concentration, using Prism software to fit a binding curve to the data point using the "one site specific" binding option. All MST measurements were performed in triplicate, with each set of experiments including a negative control to rule out nonspecific binding. For binding inhibition and recovery studies, 5 mM EDTA in the presence or absence of 10 mM  $MgCl_2$  or 20 mM  $ZnCl_2$  were added to the binding buffer and preincubated with the purified CRISP2 protein before measuring binding with A1BG, the Ig3 domain of A1BG, cholesterol sulfate, or palmitic acid.

### Co-immunoprecipitation analysis

For co-immunoprecipitation analysis, WT CRISP2 was tagged with an HA epitope, and the Ig domains of A1BG, Ig1, Ig3, and Ig4 were fused to a FLAG tag. Yeast strains expressing these proteins were grown overnight in yeast peptone dextrose medium buffered at pH 6.8 (75 mM phosphate/citrate) and collected by centrifugation. The culture medium was concentrated using size-exclusion spin columns (3K MWCO, Pierce, Thermo Fisher Scientific). The concentrated culture supernatant was incubated overnight at 4 °C with anti-HA magnetic beads (Pierce, Thermo Fisher Scientific). Beads were collected, washed with lysis buffer (50 mM Tris-HCl pH 7.5, 100 mM NaCl, 0.1% NP-40, 5% glycerol, protease inhibitor, and 1 mM PMSF), and eluted by the addition of 2× reducing protein sample buffer. Samples were denatured for 10 min at 95 °C and analyzed by SDS-PAGE and Western blotting. Experiments were performed in multiple replicates with similar results.

### Molecular docking

Since the tertiary structure of CRISP2 or A1BG has not yet been experimentally determined, a structure predicted by AlphaFold2 was used (66, 67). Binding of CRISP2 to A1BG was assessed using the AlphaFold tool in UCSF Chimera X (68, 69). The predicted docking sites between the two proteins were analyzed by PROtein binDing enerGY prediction and visualized using UCSF Chimera X (69, 70).

### Data availability

All data are contained within the manuscript.

**Supporting information**—This article contains supporting information (35, 38).

**Acknowledgments**—We thank Stéphanie Cottier for comments on the manuscript.

**Author contributions**—O. E. A., B. G., Z. H., J. S., O. A. A., and R. S. writing—review and editing; O. E. A., B. G., Z. H., J. S., O. A. A. and R. S. formal analysis; O. E. A., B. G., Z. H., O. A. A., J. S., and R. S. investigation; O. E. A., B. G., Z. H., J. S., and R. S. validation; O. E. A., B. G., Z. H., J. S., and R. S. visualization; O. E. A. and J. S., data curation; O. E. A., O. A. A., and R. S. conceptualization; O. E. A. methodology; R. S. supervision; R. S. funding acquisition; R. S. project administration; R. S. writing—original draft; R. S. resources.

**Funding and additional information**—This work was supported by the Swiss National Science Foundation (Grants 31003A\_173003, and 310030\_207870).

**Conflict of interest**—The authors declare that they have no conflict of interest with the content of this article.

**Abbreviations**—The abbreviations used are: A1BG, alpha-1-B glycoprotein; CA, cholesterol acetate; CRISP, cysteine-rich secretory protein; FAME, fatty acid methyl ester; HA, hemagglutinin; Ig, immunoglobulin; L98, leucine residue at position 98; MST, micro-scale thermophoresis; PSP94, prostate secretory protein of 94 amino acids; SC, synthetic complete; TCA, trichloroacetic acid.

### References

1. Gibbs, G. M., Roelants, K., and O'Bryan, M. K. (2008) The CAP superfamily: cysteine-rich secretory proteins, antigen 5, and pathogenesis-related 1 proteins—roles in reproduction, cancer, and immune defense. *Endocr. Rev.* **29**, 865–897
2. Schneiter, R., and Di Pietro, A. (2013) The CAP protein superfamily: function in sterol export and fungal virulence. *Biomol. Concepts* **4**, 519–525
3. Han, Z., Xiong, D., Schneiter, R., and Tian, C. (2023) The function of plant PR1 and other members of the CAP protein superfamily in plant-pathogen interactions. *Mol. Plant Pathol.* **24**, 651–668
4. Szyperki, T., Fernandez, C., Mumenthaler, C., and Wuthrich, K. (1998) Structure comparison of human glioma pathogenesis-related protein GliPR and the plant pathogenesis-related protein P14a indicates a functional link between the human immune system and a plant defense system. *Proc. Natl. Acad. Sci. U. S. A.* **95**, 2262–2266
5. Wang, Y. L., Kuo, J. H., Lee, S. C., Liu, J. S., Hsieh, Y. C., Shih, Y. T., et al. (2010) Cobra CRISP functions as an inflammatory modulator via a novel  $Zn^{2+}$ - and heparan sulfate-dependent transcriptional regulation of endothelial cell adhesion molecules. *J. Biol. Chem.* **285**, 37872–37883
6. Asojo, O. A., Koski, R. A., and Bonafe, N. (2011) Structural studies of human glioma pathogenesis-related protein 1. *Acta Crystallogr. D Biol. Crystallogr.* **67**, 847–855
7. Mason, L., Tribolet, L., Simon, A., von Gnielinski, N., Nienaber, L., Taylor, P., et al. (2014) Probing the equatorial groove of the hookworm protein and vaccine candidate antigen, Na-ASP-2. *Int. J. Biochem. Cell Biol.* **50**, 146–155
8. Darwiche, R., Kelleher, A., Hudspeth, E. M., Schneiter, R., and Asojo, O. A. (2016) Structural and functional characterization of the CAP domain of pathogen-related yeast 1 (Pry1) protein. *Sci. Rep.* **6**, 28838
9. Cantacessi, C., and Gasser, R. B. (2012) SCP/TAPS proteins in helminths—where to from now? *Mol. Cell Probes* **26**, 54–59
10. Darwiche, R., El Atab, O., Cottier, S., and Schneiter, R. (2018) The function of yeast CAP family proteins in lipid export, mating, and pathogen defense. *FEBS Lett.* **592**, 1304–1311
11. Lim, S., Kierzek, M., O'Connor, A. E., Brenker, C., Merriner, D. J., Okuda, H., et al. (2019) CRISP2 is a regulator of multiple aspects of sperm function and male fertility. *Endocrinology* **160**, 915–924
12. Gonzalez, S. N., Sulzyk, V., Weigel Muñoz, M., and Cuasnicu, P. S. (2021) Cysteine-rich secretory proteins (CRISP) are key players in mammalian fertilization and fertility. *Front. Cell Dev. Biol.* **9**, 800351

13. Guo, M., Teng, M., Niu, L., Liu, Q., Huang, Q., and Hao, Q. (2005) Crystal structure of the cysteine-rich secretory protein stecrisp reveals that the cysteine-rich domain has a K<sup>+</sup> channel inhibitor-like fold. *J. Biol. Chem.* **280**, 12405–12412
14. Gibbs, G. M., Scanlon, M. J., Swarbrick, J., Curtis, S., Gallant, E., Dulhunty, A. F., *et al.* (2006) The cysteine-rich secretory protein domain of Tpx-1 is related to ion channel toxins and regulates ryanodine receptor Ca<sup>2+</sup> signaling. *J. Biol. Chem.* **281**, 4156–4163
15. Gaikwad, A. S., Hu, J., Chapple, D. G., and O'Bryan, M. K. (2020) The functions of CAP superfamily proteins in mammalian fertility and disease. *Hum. Reprod. Update* **26**, 689–723
16. Kosari, F., Asmann, Y. W., Chevillat, J. C., and Vasmataz, G. (2002) Cysteine-rich secretory protein-3: a potential biomarker for prostate cancer. *Cancer Epidemiol. Biomarkers Prev.* **11**, 1419–1426
17. Mostaghel, E. A., Solomon, K. R., Pelton, K., Freeman, M. R., and Montgomery, R. B. (2012) Impact of circulating cholesterol levels on growth and intratumoral androgen concentration of prostate tumors. *PLoS One* **7**, e30062
18. Tadokoro, T., Modahl, C. M., Maenaka, K., and Aoki-Shioi, N. (2020) Cysteine-rich secretory proteins (CRISPs) from venomous snakes: an overview of the functional diversity in a large and underappreciated superfamily. *Toxins (Basel)* **12**, E175
19. Schultze, H. E., Heide, K., and Haupt, H. (1963) Isolation of an easily precipitable alpha1-glycoprotein of human serum. *Nature* **200**, 1103
20. Clerc, F., Reiding, K. R., Jansen, B. C., Kammeijer, G. S., Bondt, A., and Wührer, M. (2016) Human plasma protein N-glycosylation. *Glycoconj. J.* **33**, 309–343
21. Ishioka, N., Takahashi, N., and Putnam, F. W. (1986) Amino acid sequence of human plasma alpha 1B-glycoprotein: homology to the immunoglobulin supergene family. *Proc. Natl. Acad. Sci. U. S. A.* **83**, 2363–2367
22. Bork, P., Holm, L., and Sander, C. (1994) The immunoglobulin fold. Structural classification, sequence patterns and common core. *J. Mol. Biol.* **242**, 309–320
23. Youkharibache, P. (2021) Topological and structural plasticity of the single Ig fold and the double Ig fold present in CD19. *Biomolecules* **11**, 1290
24. Yoon, S. Y., Kim, J. M., Oh, J. H., Jeon, Y. J., Lee, D. S., Kim, J. H., *et al.* (2006) Gene expression profiling of human HBV- and/or HCV-associated hepatocellular carcinoma cells using expressed sequence tags. *Int. J. Oncol.* **29**, 315–327
25. Tian, M., Cui, Y. Z., Song, G. H., Zong, M. J., Zhou, X. Y., Chen, Y., *et al.* (2008) Proteomic analysis identifies MMP-9, DJ-1 and A1BG as overexpressed proteins in pancreatic juice from pancreatic ductal adenocarcinoma patients. *BMC Cancer* **8**, 241
26. Kreunin, P., Zhao, J., Rosser, C., Urquidí, V., Lubman, D. M., and Goodison, S. (2007) Bladder cancer associated glycoprotein signatures revealed by urinary proteomic profiling. *J. Proteome Res.* **6**, 2631–2639
27. Piyaphanee, N., Ma, Q., Kremen, O., Czech, K., Greis, K., Mitsnefes, M., *et al.* (2011) Discovery and initial validation of  $\alpha$  1-B glycoprotein fragmentation as a differential urinary biomarker in pediatric steroid-resistant nephrotic syndrome. *Proteomics Clin. Appl.* **5**, 334–342
28. Liu, Y., Luo, X., Hu, H., Wang, R., Sun, Y., Zeng, R., *et al.* (2012) Integrative proteomics and tissue microarray profiling indicate the association between overexpressed serum proteins and non-small cell lung cancer. *PLoS One* **7**, e51748
29. Biswas, S., Sharma, S., Saroha, A., Bhakuni, D. S., Malhotra, R., Zahur, M., *et al.* (2013) Identification of novel autoantigen in the synovial fluid of rheumatoid arthritis patients using an immunoproteomics approach. *PLoS One* **8**, e56246
30. Cordeiro, Y. G., Mulder, L. M., van Zeijl, R. J. M., Paskoski, L. B., van Veelen, P., de Ru, A., *et al.* (2021) Proteomic analysis identifies FNDC1, A1BG, and antigen processing proteins associated with tumor Heterogeneity and malignancy in a canine model of breast cancer. *Cancers (Basel)* **13**, 5901
31. Zeng, Z., Hincapie, M., Haab, B. B., Hanash, S., Pitteri, S. J., Kluck, S., *et al.* (2010) The development of an integrated platform to identify breast cancer glycoproteome changes in human serum. *J. Chromatogr. A.* **1217**, 3307–3315
32. Udby, L., Sorensen, O. E., Pass, J., Johnsen, A. H., Behrendt, N., Borregaard, N., *et al.* (2004) Cysteine-rich secretory protein 3 is a ligand of alpha1B-glycoprotein in human plasma. *Biochemistry* **43**, 12877–12886
33. Udby, L., Johnsen, A. H., and Borregaard, N. (2010) Human CRISP-3 binds serum alpha(1)B-glycoprotein across species. *Biochim. Biophys. Acta* **1800**, 481–485
34. Choudhary, V., and Schneider, R. (2012) Pathogen-Related Yeast (PRY) proteins and members of the CAP superfamily are secreted sterol-binding proteins. *Proc. Natl. Acad. Sci. U. S. A.* **109**, 16882–16887
35. El Atab, O., Kocabay, A. E., Asojo, O. A., and Schneider, R. (2022) Prostate secretory protein 94 inhibits sterol binding and export by the mammalian CAP protein CRISP2 in a calcium-sensitive manner. *J. Biol. Chem.* **298**, 101600
36. Lewis, T. A., Taylor, F. R., and Parks, L. W. (1985) Involvement of heme biosynthesis in control of sterol uptake by *Saccharomyces cerevisiae*. *J. Bacteriol.* **163**, 199–207
37. Jacquier, N., and Schneider, R. (2012) Mechanisms of sterol uptake and transport in yeast. *J. Steroid Biochem. Mol. Biol.* **129**, 70–78
38. Tiwari, R., Koffel, R., and Schneider, R. (2007) An acetylation/deacetylation cycle controls the export of sterols and steroids from *S. cerevisiae*. *EMBO J.* **26**, 5109–5119
39. Wienken, C. J., Baaske, P., Rothbauer, U., Braun, D., and Duhr, S. (2010) Protein-binding assays in biological liquids using microscale thermophoresis. *Nat. Commun.* **1**, 100
40. Jerabek-Willemsen, M., André, T., Wanner, R., Roth, H. M., Duhr, S., Baaske, P., *et al.* (2014) MicroScale thermophoresis: interaction analysis and beyond. *J. Mol. Struct.* **1077**, 101–113
41. El Atab, O., and Schneider, R. (2023) Measuring the interaction of sterols and steroids with proteins by microscale thermophoresis. *Methods Mol. Biol.* **2704**, 173–181
42. Xu, X., Francischetti, I. M., Lai, R., Ribeiro, J. M., and Andersen, J. F. (2012) Structure of protein having inhibitory disintegrin and leukotriene scavenging functions contained in single domain. *J. Biol. Chem.* **287**, 10967–10976
43. Choudhary, V., Darwiche, R., Gfeller, D., Zoete, V., Michielin, O., and Schneider, R. (2014) The caveolin-binding motif of the pathogen-related yeast protein Pry1, a member of the CAP protein superfamily, is required for *in vivo* export of cholesteryl acetate. *J. Lipid Res.* **55**, 883–894
44. Darwiche, R., Mène-Saffrané, L., Gfeller, D., Asojo, O. A., and Schneider, R. (2017) The pathogen-related yeast protein Pry1, a member of the CAP protein superfamily, is a fatty acid-binding protein. *J. Biol. Chem.* **292**, 8304–8314
45. Scharnewski, M., Pongdontri, P., Mora, G., Hoppert, M., and Fulda, M. (2008) Mutants of *Saccharomyces cerevisiae* deficient in acyl-CoA synthetases secrete fatty acids due to interrupted fatty acid recycling. *FEBS J.* **275**, 2765–2778
46. Ekim Kocabay, A., and Schneider, R. (2023) Human lipocalins bind and export fatty acids through the secretory pathway of yeast cells. *Front. Microbiol.* **14**, 1309024
47. Jumperet, J., Evans, R., Pritzel, A., Green, T., Figurnov, M., Ronneberger, O., *et al.* (2021) Highly accurate protein structure prediction with AlphaFold. *Nature* **596**, 583–589
48. Cottier, S., Darwiche, R., Meyenhofer, F., Debelyy, M. O., and Schneider, R. (2020) The yeast cell wall protein Pry3 inhibits mating through highly conserved residues within the CAP domain. *Biol. Open* **9**, bio053470
49. Oreste, U., Ametrano, A., and Coscia, M. R. (2021) On origin and evolution of the antibody molecule. *Biology (Basel)* **10**, 140
50. Catanese, J. J., and Kress, L. F. (1992) Isolation from opossum serum of a metalloproteinase inhibitor homologous to human alpha 1B-glycoprotein. *Biochemistry* **31**, 410–418
51. Qi, Z. Q., Yonaha, K., Tomihara, Y., and Toyama, S. (1995) Isolation of peptides homologous to domains of human alpha 1B-glycoprotein from a mongoose antihemorrhagic factor. *Toxicon* **33**, 241–245
52. Neves-Ferreira, A. G., Perales, J., Fox, J. W., Shannon, J. D., Makino, D. L., Garratt, R. C., *et al.* (2002) Structural and functional analyses of DM43, a

- snake venom metalloproteinase inhibitor from *Didelphis marsupialis* serum. *J. Biol. Chem.* **277**, 13129–13137
53. Rocha, S. L., Lomonte, B., Neves-Ferreira, A. G., Trugilho, M. R., Junqueira-de-Azevedo, I. L., Ho, P. L., *et al.* (2002) Functional analysis of DM64, an antimitotoxic protein with immunoglobulin-like structure from *Didelphis marsupialis* serum. *Eur. J. Biochem.* **269**, 6052–6062
54. Perales, J., Neves-Ferreira, A. G., Valente, R. H., and Domont, G. B. (2005) Natural inhibitors of snake venom hemorrhagic metalloproteinases. *Toxicon* **45**, 1013–1020
55. Holding, M. L., Drabek, D. H., Jansa, S. A., and Gibbs, H. L. (2016) Venom resistance as a Model for understanding the molecular basis of complex coevolutionary adaptations. *Integr. Comp. Biol.* **56**, 1032–1043
56. Tasoulis, T., and Isbister, G. K. (2023) A current perspective on snake venom composition and constituent protein families. *Arch. Toxicol.* **97**, 133–153
57. Han, Z., and Schneider, R. (2024) Dual functionality of pathogenesis-related proteins: defensive role in plants *versus* immunosuppressive role in pathogens. *Front. Plant Sci.* **15**, 1368467
58. Arbuckle, K., Rodríguez de la Vega, R. C., and Casewell, N. R. (2017) Coevolution takes the sting out of it: evolutionary biology and mechanisms of toxin resistance in animals. *Toxicon* **140**, 118–131
59. Yamazaki, Y., and Morita, T. (2004) Structure and function of snake venom cysteine-rich secretory proteins. *Toxicon* **44**, 227–231
60. Zhou, Q., Wang, Q. L., Meng, X., Shu, Y., Jiang, T., Wagenknecht, T., *et al.* (2008) Structural and functional characterization of ryanodine receptor-natriin toxin interaction. *Biophys. J.* **95**, 4289–4299
61. Shioi, N., Tadokoro, T., Shioi, S., Okabe, Y., Matsubara, H., Kita, S., *et al.* (2019) Crystal structure of the complex between venom toxin and serum inhibitor from Viperidae snake. *J. Biol. Chem.* **294**, 1250–1256
62. van Thiel, J., Khan, M. A., Wouters, R. M., Harris, R. J., Casewell, N. R., Fry, B. G., *et al.* (2022) Convergent evolution of toxin resistance in animals. *Biol. Rev. Camb. Philos. Soc.* **97**, 1823–1843
63. Halimi, H., and Farjadian, S. (2022) Cholesterol: an important actor on the cancer immune scene. *Front. Immunol.* **13**, 1057546
64. Scheinberg, T., Mak, B., Butler, L., Selth, L., and Horvath, L. G. (2023) Targeting lipid metabolism in metastatic prostate cancer. *Ther. Adv. Med. Oncol.* **15**. <https://doi.org/10.1177/17588359231152839>
65. Horvath, A., and Riezman, H. (1994) Rapid protein extraction from *Saccharomyces cerevisiae*. *Yeast* **10**, 1305–1310
66. Bryant, P., Pozzati, G., and Elofsson, A. (2022) Improved prediction of protein-protein interactions using AlphaFold2. *Nat. Commun.* **13**, 1265
67. Gao, M., Nakajima An, D., Parks, J. M., and Skolnick, J. (2022) AF2Complex predicts direct physical interactions in multimeric proteins with deep learning. *Nat. Commun.* **13**, 1744
68. Mirdita, M., Schütze, K., Moriwaki, Y., Heo, L., Ovchinnikov, S., and Steinegger, M. (2022) ColabFold: making protein folding accessible to all. *Nat. Methods* **19**, 679–682
69. Pettersen, E. F., Goddard, T. D., Huang, C. C., Meng, E. C., Couch, G. S., Croll, T. I., *et al.* (2021) UCSF ChimeraX: structure visualization for researchers, educators, and developers. *Protein Sci.* **30**, 70–82
70. Vangone, A., and Bonvin, A. M. (2015) Contacts-based prediction of binding affinity in protein-protein complexes. *Elife* **4**, e07454